WiFall: Device-Free Fall Detection by Wireless Networks

Yuxi Wang, *Student Member, IEEE*, Kaishun Wu, *Member, IEEE*, and Lionel M. Ni, *Fellow, IEEE*

Abstract—Injuries that are caused by falls have been regarded as one of the major health threats to the independent living for the elderly. Conventional fall detection systems have various limitations. In this work, we first look for the correlations between different radio signal variations and activities by analyzing radio propagation model. Based on our observation, we propose WiFall, a truly unobtrusive fall detection system. WiFall employs physical layer Channel State Information (CSI) as the indicator of activities. It can detect fall of the human without hardware modification, extra environmental setup, or any wearable device. We implement WiFall on desktops equipped with commodity 802.11n NIC, and evaluate the performance in three typical indoor scenarios with several layouts of transmitter-receiver (Tx-Rx) links. In our area of interest, WiFall can achieve fall detection for a single person with high accuracy. As demonstrated by the experimental results, WiFall yields 90 percent detection precision with a false alarm rate of 15 percent on average using a one-class SVM classifier in all testing scenarios. It can also achieve average 94 percent fall detection precisions with 13 percent false alarm using Random Forest algorithm.

Index Terms—Wireless, channel state information, fall detection, device-free, machine learning

1 Introduction

Falls, which can be depicted as the abrupt change of human body from an upright position to a lying-down position without control [1], are prevalent among the elderly. According to the data from the Center for Disease Control and Prevention [2], one out of three adults aged 65 or older falls at least once each year. A large number of fatal injuries are caused by falls. Since reducing the rescue time after fall detection can extremely increase the overall survival of the elderly, it is necessary to deploy automatic fall detection system in home environment.

Based on monitoring instruments, existing fall detection (FD) systems can be categorized into four classes: ambient device, camera, wearable sensor and smartphone. FD systems using ambient devices [3], [4] leverage floor vibration caused by a fall to detect a risky situation. Specific devices must be implanted beforehand. System in [3] need a Piezo Transducer to build a floor vibration based fall detector, and the system in [4] needs to deploy floor sensors. FD systems using cameras [5], [6] employ activity classification algorithms on a series of images recorded by high resolution cameras, and can effectively detect a fall. However, cameras are expensive and violate personal privacy sometimes. Both wearable sensor based [7] and smartphone based [8] FD techniques employ sensors to sense the changes in acceleration or velocity on three coordinate axes. However, carrying sensors or smartphones is cumbersome for the user, and different positions (e.g., placed at chest, waist, thigh, arms, legs, etc.) of the sensors will show different detection performance. For example, the user of system in [7] needs to carry a custom-made device which comprises of accelerometer, micro-controller and other sensors during fall detection. Using PerFallD in [8], the user only needs a smartphone on him, but the position where the smartphone placed will affect the detection accuracy.

To achieve effective automatic fall detection, we require the system to be accurate, inexpensive, and user friendly. Few of the FD systems using techniques above have been widely deployed into home settings due to the fact that they suffer terrible performance when considering one or more of the above three conditions. We want to employ a new technique to conduct fall detection in order to balance the three conditions. The widespread dissemination of the wireless local area networks (WLAN) has enabled the possibility of WLAN-based fall detection in indoor environment for the elderly. WLAN infrastructures can support high-accuracy-low-cost fall detection with simple infrastructure deployment, engaging user experience and limited privacy concerns. Thus, we aim to investigate whether automatic fall detection can be achieved without any special wearable device by leveraging current commercial wireless products by exploiting the properties of WiFi signal during propagation. In the last decade, WiFi facilities and techniques have motivated a variety of research interests in localization [9], motion detection [10] and object tracking [11]. Currently, more research works have addressed the relationship between wireless signals and human activities.

In order to implement unobtrusive fall detection by wireless networks, we need to find a good representation of the wireless signal. It should be robust to environmental changes but sensitive to human disturbances. However, we observe that current radio propagation model cannot be

- *Y. Wang and K. Wu are with the College of Computer Science and Software Engineering, Shenzhen University, P.R. China, and the CSE Department, Hong Kong University of Science and Technology (HKUST), Kowloon, Hong Kong. E-mail: ywangav@cse.ust.hk, wu@szu.edu.cn.*
- *L. M. Ni is with the Department of Computer and Information Science, University of Macau, Taipa, Macau, China. E-mail: ni@umac.mo.*

Manuscript received 13 July 2015; revised 14 Mar. 2016; accepted 13 Apr. 2016. Date of publication 22 Apr. 2016; date of current version 5 Jan. 2017.
For information on obtaining reprints of this article, please send e-mail to: reprints@ieee.org, and reference the Digital Object Identifier below.
Digital Object Identifier no. 10.1109/TMC.2016.2557792

applied directly when considering complex human activities. Therefore, it is difficult to observe the relationship between human activities and wireless signal properties based on existing radio propagation models.

In this paper, we first address the wireless radio propagation model in indoor environments under the disturbances of human activities. We analyze the radio propagation model during falling from theoretical perspective, and present a refined model when the user is at the NLOS location. Based on our theoretical case study, we propose WiFall, a passive device-free fall detection system leveraging Channel State Information (CSI) as the indicator. We define the area which can be covered by the signal communication links of WiFall for fall detection as the effective range area for performance evaluation, and it is our area of interest. WiFall can detect various activities for a single person inside the effective range area, and can achieve fall detection with high accuracy. In summary, the main contributions of this paper are as follows:

- We exploit the feasibility of using fine-grained Channel State Information for device-free fall detection for a single person. We take temporal stability and frequency diversity of CSI to design WiFall, a passive device-free fall detection system. Compared with other FD systems, WiFall leverages existing prevalent wireless infrastructures, and can be widely deployed into real life with low cost.
- To realize truly unobtrusive fall detection, we present a case study from theoretical perspective by taking human activities into consideration. On the basis of motion detection by anomaly detection algorithm, we apply a one-class Support Vector Machine classifier and Random Forest algorithm to classify different human activities and achieve fall detection.
- Extensive evaluations of WiFall with commodity 802.11n NICs equipped on laptops are conducted in three typical indoor scenarios with different Tx-Rx layout schemes. The measurements show that WiFall can achieve an average detection accuracy of 94 percent with Random Forest-based classification in all testing scenarios. Furthermore, WiFall can be extended for identification of other human activities.

The rest of this paper is organized as follows. We will present the related work of WiFall in Section 2, and we will introduce the background knowledge in Section 3. Then in Section 4, we will introduce the detailed design of our WiFall system. Section 5 will describe the methods to evaluate the WiFall system, followed by the evaluation results in Section 6. Finally, we will give our conclusions and discussions on WiFall in Section 7.

2 Related Work

WiFall is closely related to the following three research categories:

Wireless motion detection. Motion detection is the detection of the movement of entities in an area of interest. Noury et al. [1], Yu [12] and Mubashir et al. [13] review the principles and approaches used in existing fall detection (FD) systems. In [14], the authors propose an innovative approach called Wi-Vi. It can track the moving path of a human but cannot detect specific activities using wireless signals. In [15], the authors introduce WiTrack which can track the 3D motion of a target person. The updated version of this work called WiTrack2.0 [16] achieves 3D motion tracking of multiple targets. Both WiTrack and WiTrack2.0 can detect falling of a person with wireless signals. However, these two approaches are implemented using USRP/GNURadio with daughter boards, and cannot be implemented by commercial products. With advanced wireless devices, more subtle movements can be detected. Authors in [17] propose a method named WiSee to conduct gesture recognition. WiSee can classify nine whole-body gestures by analyzing the Doppler shifts of wireless signals extracted during transmission. RSS obtained from commercial wireless product can also be applied for activity detection such as gesture recognition [18]. Yet, RSS is consider to be not reliable in a cluttered environment due to multipath. Therefore, a fine-grained indicator Channel State Information attracts researcher's attentions. CSI has also been utilized for wireless motion detection. FIMD [10] is a system which can monitor the motion behavior of the target using CSI extracted from commodity WiFi NIC. In our work, we not only focus on motion detection, but identify specific human activities. We only leverage commodity WiFi products to detect the motion of the target using CSI. Compared with systems using specific-designed wireless devices and RSS, WiFall can achieve satisfactory detection accuracy and can be more widely deployed in real indoor environment with low cost.

CSI-based activity identification. Since CSI has been verified to be a reliable indicator for device-free wireless motion detection, more researchers seek for the opportunity to identify various activities using CSI-based feature. Our system WiFall [19] is prior work among these systems. It learns specific CSI signal amplitude patterns using machine learning algorithms, and distinguishes falling from other movements. Instead of using CSI amplitude directly for activity recognition, E-eyes [20] utilizes the distribution of CSI amplitude to classify the activities in whole home environment. The activities identified by the system have high correlations with the locations. The authors in [21] observe that radio frequency interference (RFI) has a significant impact on CSI vectors, and introduce a device-free location-oriented activity system based on their observation. In [22], the authors propose another CSI-based human activity monitoring system called CARM. CARM contains a CSI-speed model which transfer CSI amplitude variation caused by human movements into speed information. Based on the fact that different human movements will cause different speed changes, CARM quantifies the correlation between speed and movement, and recognizes a given activity with Hidden Markov Model. It is a remarkable work in CSI-based activity recognition. CSI from commercial off-the-shelf (COTS) WiFi devices can also be leveraged for subtle movement recognition, such as gesture recognition [23], keystroke tracking [24] and in-air drawing [25]. In this paper, we improve our WiFall system in [19]. Different from other activity identification systems, we mainly focus on activity recognition of the elderly, who belong to a relatively special social group with obvious common behaviors. It is designed for healthcare scenarios. We revise our method to improve the detection accuracy and implement the complete WiFall system.

Device-free indoor localization. Another important technique related to WiFall is device-free indoor localization. Authors in [26] first describe device-free passive (DfP) localization, which does not require the entities to carry any device during positioning. Mainstream systems leverage fingerprinting method to locate the tracked entity, and RSS is the most widely used fingerprint. Nuzzer [27] is a representative work, which estimates the location of the target by comparing RSS to the fingerprint stored in a beforehand passive radio map. The system ACE [28] solves the problem of positioning multiple entities using a probabilistic energy-minimization framework. After CSI has been leveraged for device-based indoor localization such as FILA [9], [29] and MODLoc [30], more efforts have been paid in device-free scenarios. Different from RSS-based system, the passive radio map in CSI-based system is constructed using CSI matrices. Pilot [31] is known to be a prior work using CSI for device-free indoor localization. It first examines whether a target is present in the area of interest, and then estimates the location by mapping the abnormal CSI caused by the target to fingerprint in radio map. MonoPHY [32] is a DfP localization system which only utilizes one single stream of CSI for positioning. Authors in [33] find that receivers at different locations possess diverse sensitivity to environment changes, and they utilize this observation to improve localization accuracy. Similar to DfP indoor localization which leverages the fact that RSS or CSI will change when the horizontal position of the object changes, we track and analyze the effects of vertical position variations of the object person on CSI to achieve device-free fall detection.

3 Preliminaries

In this section, we will present the background knowledge of WiFall system, and give a case study on the signal variation during falling from theoretical perspective.

3.1 Channel State Information

Channel State Information or Channel Status Information (CSI) is information that estimates the channel properties of a communication link [34]. In wireless communication, a transmitted radio signal is affected by the physical environment (e.g., reflection, diffraction and scattering). CSI describes how a signal propagates in the channel by combining the effects of time delay, amplitude attenuation and phase shift. In frequency domain, the narrowband flat-fading channel with multiple transmission and receiving antennas (multi-input-multi-output, MIMO) is modeled as:

$$y = Hx + n, \tag{1}$$

where y is the received vector, x is the transmitted vector, n is the noise vector, and H is the channel matrix. As noise is often modeled as circular symmetric complex normal with $n \sim cN(0, S)$, H in the above formula can be estimated as:

$$\hat{H} = \frac{y}{x}.$$

CSI is an estimation of H. In Orthogonal Frequency Division Multiplexing (OFDM) system, CSI is represented at subcarrier level. CSI of a single subcarrier is in the following mathematical format:

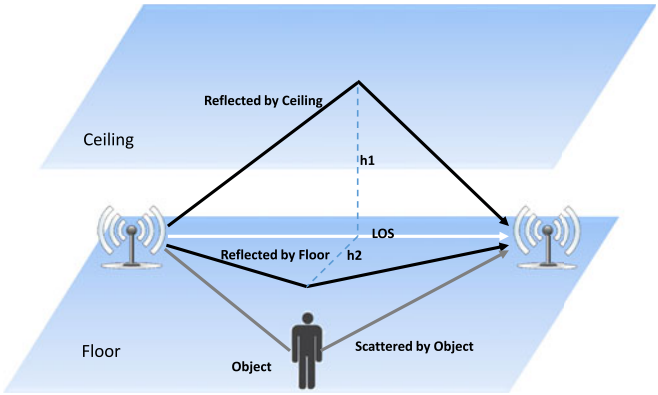

Fig. 1. Signal propagation model in indoor environment.

$$h = |h|e^{jsin\theta},$$

where $|h|$ is the amplitude and θ is the phase of each subcarrier.

CSI provides a finer-grained representation of the wireless link compared with Received Signal Strength (RSS). Thus, recent wireless applications tend to employ CSI rather than RSS. We will give experimental analysis about how to leverage CSI to indicate human activities.

3.2 Propagation Model for Falling: A Case Study

The idea of device-free fall detection using CSI is based on the fact that human presence and movement will affect the propagation paths of wireless signals. In this section, we provide a case study when falling happens at a NLOS location with theoretical analysis. We only consider activities happen at a fixed location and name these activities as in-place activities (falling, sitting down, and standing up). The model in this section proves that falling can be distinguished using wireless signals from theoretical perspective.

In a typical indoor environment, there is one main path (Line-Of-Sight, LOS) and several reflected paths (None-Line-Of-Sight, NLOS) due to the surroundings such as ceiling, floor and walls, as shown in Fig. 1. The LOS path suffers from free space path loss. According to the free space model, the received power by a receiver antenna which is separated from a radiating transmitter antenna by a distance d, is given by the Friis free space equation [34]:

$$P_{los}(d) = \frac{P_t G_t G_r \lambda^2}{(4\pi)^2 d^2}, \tag{2}$$

where P_t is the transmitted power, $P_{los}(d)$ is the received power which is a function of the distance d, G_r is the receiving antenna gain, G_t is the transmitter antenna gain, λ is the wavelength in meters and d is the distance from transmitter to receiver in meters.

Consider the scenario that paths deflected off the walls are ignored, when the transmitter and receiver are placed near the ground, the power received by the receiver through ceiling and ground paths can be represented as [11]:

$$P_{ceil}(d) = \frac{P_t G_t G_r \lambda^2}{(4\pi)^2 (d^2 + 4{h_1}^2)}, \tag{3}$$

$$P_{floor}(d) = \frac{P_t G_t G_r \lambda^2}{(4\pi)^2 (d^2 + 4{h_2}^2)}, \tag{4}$$

where h_1 and h_2 are the distance from ceiling or floor to the transmitter-receiver (Tx-Rx) link, respectively.

When the target presents in this static environment, there will several scattered paths caused by the human body. According to the radar equation [35], the received power influenced by the target is computed as:

$$P_{sca}(r_1, r_2) = \sum_{h_i} \frac{P_t G_t G_r \lambda^2 \sigma}{(4\pi)^3 (r_1^2 + h_i^2)(r_2^2 + h_i^2)} \quad h_i \in (0, h], \quad (5)$$

where r_1 is the distance from the transmitter to the target, and r_2 is the distance from the receiver to the target in horizontal plane. h_i represents the height of the scattered points, and h is the height of the target.

Suppose the intensity magnitudes of LOS, ceiling, ground and scattered paths are E_{los}, E_{ceil}, E_{floor} and E_{sca}, respectively. The total received power by the receiver can be computed as:

$$P \propto |E_{los} + E_{ceil} + E_{floor} + E_{sca}|^2. \quad (6)$$

When the target falls, E_{los}, E_{ceil} and E_{floor} remain unchanged, the changes in the received scattered power at the receiver can be represented as:

$$\Delta P_{sca} = \sum_{h_i} \frac{P_t G_t G_r \lambda^2 \sigma}{(4\pi)^3 (r_1^2 + h_i^2)(r_2^2 + h_i^2)} \quad h_i \in (h - \delta, h], \quad (7)$$

where δ is the reduced height of human body due to the fall. Therefore, there will be significant change in E_{sca} and the total received power P. Other in-place activities will also cause the change of P. We analyze the energy changes when conducting falling and sitting down at the location $1m$ away from the AP-MP link in the lab. Our experimental data show that the maximum energy change during falling is $21.3dB$ and the time duration of variation is around $1s$. The energy vibrates for more than $4s$ when the person sits down, and the maximum energy change is $9.31dB$. Consider energy change and time duration, the energy variation during falling is more obvious than that when other in-place activities (e.g., sitting down) occur. The energy change is closely related to the environment, the setting of AP-MP link, and the location to perform activities. Therefore, the energy change of each activity is not a fixed value. We do not simply quantify the energy change but analyze the energy variation based on the model with learning method when we design the WiFall system.

4 WiFall System

In this section, we first introduce the architecture of WiFall. Then we depict the major modules in WiFall system in details.

4.1 System Overview

WiFall leverages CSI to indicate human activities in an indoor environment, and then learns the specific patterns related to fall and other focused activities. Fig. 2 presents an overview of the system. The WiFall system consists of three main phases: sensing, learning, and alerting.

In the sensing phase, the transmitter (Access Point, AP) propagates wireless signals. The receiver (Monitoring Point, MP) in the same area of interest collects the wireless physical information CSIs, and sends them to the next phase.

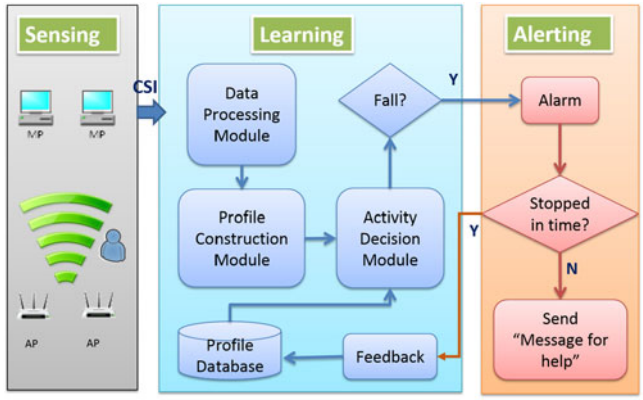

Fig. 2. Overview of system architecture.

Learning phase contains three important modules: data processing, profile construction, activity decision module. We obtain CSI profiles from the CSI data which have been denoised and reconstructed. The profiles collected during training process are stored in the profile database, and the profiles gathered during testing process are utilized for activity decision by applying two machine algorithms.

In the final phase alerting, an emergency alarm is triggered when falling is detected. The application will pop up an alarm and send message for help if the alarm has not been stopped in time. The false alarm data can be used to give feedback to the learning phase in order to update the profile database.

4.2 Data Processing

CSIs are extracted from received packages in MPs. Using the CSI tool introduced in [36], the CSI packet received is a $N_{tx} \times N_{rx} \times 30$ matrix, where N_{tx} is the antenna number for AP, N_{rx} is the antenna number for MP, and the third dimension is across 30 subcarriers in the OFDM channel. Let $N_{tx} = 3$ and $N_{rx} = 3$, a CSI packet contains 9 streams with 30 subcarriers in each stream, which can be represented in the following format:

$$\begin{aligned} CSI^1 &= \{CSI^{1,1}, CSI^{1,2}, \ldots, CSI^{1,30}\} \\ CSI^2 &= \{CSI^{2,1}, CSI^{2,2}, \ldots, CSI^{2,30}\} \\ &\cdots\cdots\cdots \\ CSI^9 &= \{CSI^{9,1}, CSI^{9,2}, \ldots, CSI^{9,30}\}, \end{aligned}$$

where in $CSI^{i,j}$, i is the stream number and j is the subcarrier number.

In WiFall, we take the amplitude of CSI for activity classification, and leave phase information for our future work. The CSI mentioned in the rest of paper means the CSI amplitude. Previously, we discover that human movements affect the nine streams differently whereas the 30 subcarriers similarly, as shown in Figs. 3 and 4. By computing the correlation matrix of CSI subcarriers, we observe that all the subcarriers have positive correlation and the correlation ratios between successive subcarriers are high. We present the correlation matrix of Subcarrier 1 to Subcarrier 30, shown in Fig. 5. Based on the observations, we try to aggregate CSI of 30 subcarriers into one single value CSI^i.

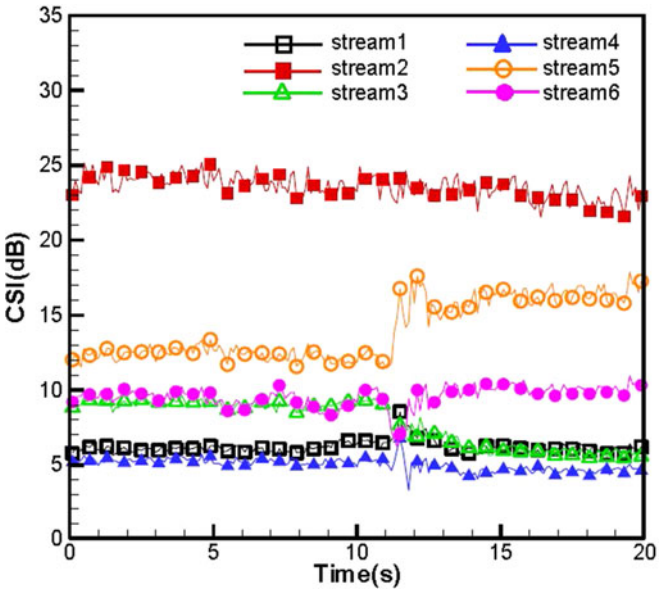

Fig. 3. CSI variances of 1st subcarrier in different streams.

The CSI for each stream is aggregated using the following equation in [9]:

$$CSI^{i} = \frac{1}{N}\sum_{j=1}^{N}\frac{f_j}{f_0} \times |CSI^{i,j}|, \tag{8}$$

where f_0 is the central frequency. Therefore, the previous CSI data for each time slot t we use is a 9-column array as follows:

$$CSIS_t = \left[CSI_t^1, CSI_t^2, \ldots, CSI_t^9\right].$$

However, we observe that the aggregation partially loses the frequency diversity of CSI subcarriers especially in environment with rich multipath. Therefore, we reconstruct the CSI packet at time t into:

$$CSI_t = \left[CSI_t^{1,1}, CSI_t^{2,1}, \ldots, CSI_t^{9,1}, CSI_t^{1,2}, \ldots, CSI_t^{8,30}, CSI_t^{9,30}\right],$$

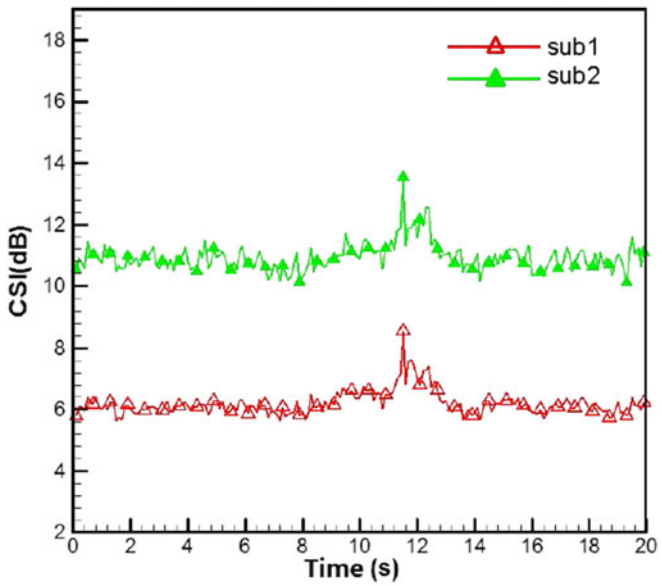

Fig. 4. CSI variances of different subcarriers in one stream.

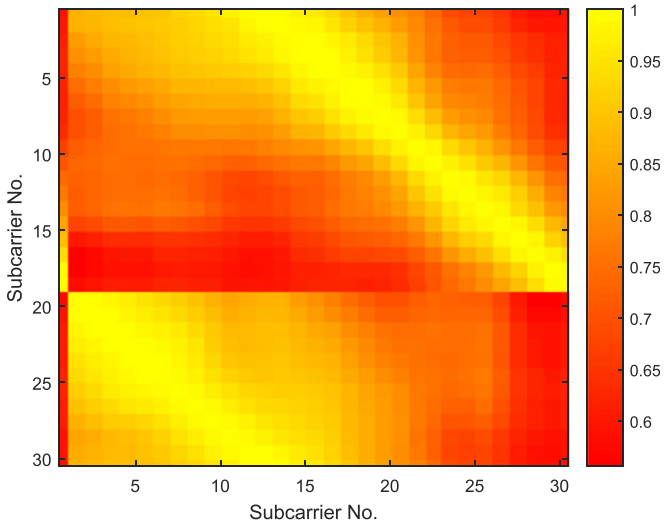

Fig. 5. Correlation matrix of CSI subcarriers in one stream.

which is an array with 270 columns. We apply the new constructed 270-column arrays for fall identification. The 9-column arrays $CSIS_t$s are only used in anomaly detection.

Environmental factors such as temperature and room settings may also cause a fluctuation in the received CSI. WiFall reduces environmental noise by employing a weighted moving average filter. For example, the 270-column CSI value at time t is averaged by the equation:

$$\widehat{CSI_t} = \frac{1}{m + (m-1) + \cdots + 1} \times (m \times CSI_t + (m-1) \times CSI_{t-1} + \cdots + 1 \times CSI_{t-m+1}). \tag{9}$$

The value of m decides to what degree the current value is related with the historical records. The reconstructed CSI matrix is processed for profile construction. Similarly, the 9-column CSI arrays are denoised using the weighted moving average filter before anomaly detection.

4.3 Profile Construction

In this part, we introduce the techniques we used to build our CSI profile for fall detection.

4.3.1 Anomaly Detection

Anomaly detection aims to detect the anomaly change in wireless signal. The activities that WiFall system focuses are walking, sitting down, standing up and falling. Although various immobile human postures result in different signal power at MPs, they have similar signal changing patterns in time domain, which are steady over the time. Using a Local Outlier Factor based anomaly detection algorithm, WiFall picks out human activities and isolates the corresponding anomaly patterns.

In this step, the system learns a model of stable situation. For a given series of CSI data, we compute LOF of the data compared with the stable model in order to detect anomaly patterns. We define a situation is stable when the person present in the area of interest is resting. The stable profile is extracted before WiFall system conducts detection work, and it evaluates the stable wireless signal propagation features without any human activities.

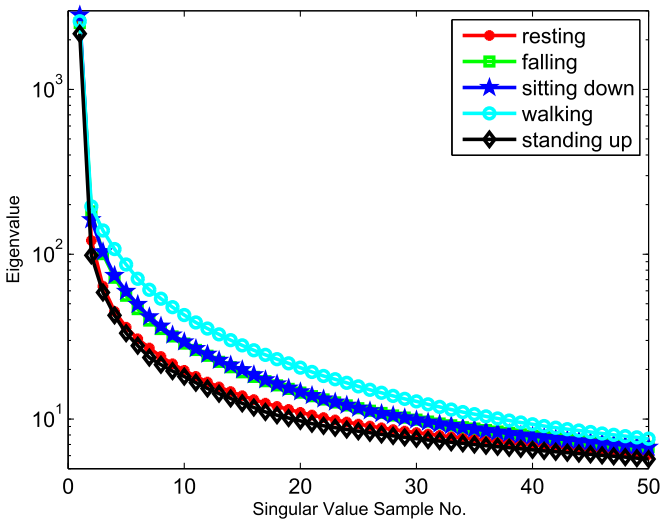

Fig. 6. Eigenvalues of SVD matrix.

Given $\mathbf{CSI}^i = \{CSI_1^i, CSI_2^i, \ldots, CSI_n^i\}$ which is a series of CSI of stream i, the approximated density function $\hat{p}(x)$ is computed as:

$$\hat{p}(x) = \frac{1}{n}\sum_{t=1}^{n} \delta_n(x - CSI_t^i), \tag{10}$$

where n is the number of CSI and $\delta_n(\cdot)$ is a kernel function. According to [37], the local density is estimated by a specific distance at which a sample point can be reached from its neighbors. Concretely, the local density of a point p, which is $lrd(p)$, is defined as:

$$lrd(p) = 1/\frac{\sum_{o\in k(p)} reach - dist_k(p,o)}{k}, \tag{11}$$

where $k(p)$ is the set of k-nearest neighbor of p, o is any selected point in $k(p)$, k is the number of chosen nearest neighbors, $reach - dist_k(p,o)$ is called reachability distance. Let $k - distance(p)$ be the distance of object p to the k nearest neighbors and $d(p,o)$ be the distance from p to o, $reach - dist_k(p,o)$ can be calculated as

$$reach - dist_k(p,o) = max(k - distance(p), d(p,o)). \tag{12}$$

Local Outlier Factor is defined as the ratio of average local densities of one object's neighbors to the local density of the object. LOF of point p is computed as follows:

$$LOF(p) = \frac{\frac{1}{k}\sum_{o\in k(p)} lrd(o)}{lrd(p)}. \tag{13}$$

We consider each stream of CSI one input of the LOF function, and compute the LOF values of the CSI samples. Therefore, we will obtain 9 LOF lists as the result of a CSI dataset. LOF denotes the probability of whether a point is an outlier or not. An LOF value of approximately 1 indicates that the point is located in a region of homogeneous density, and is not an outlier. In each stream, if there is an outlier occurs, we believe the stream is anomaly. For all the nine streams, if majority of the streams show anomaly features, we believe that the activity corresponding to the CSI dataset is anomaly.

TABLE 1
Proportion of Top Three Eigenvalues in SVD Matrix

	Proportion
resting	99.92%
falling	99.83%
sitting down	99.86%
walking	99.65%
standing up	99.91%

4.3.2 SVD Matrix Factorization

After detected anomaly activities, WiFall applies classification algorithm on CSI matrix to identify activity. To decrease the processing time during classification, we leverage a Singular Value Decomposition (SVD) matrix to perform a selection on the eigenvalue of the CSI data selected by anomaly detection. SVD is a method to transform correlated variables into a set of uncorrelated variable which better exposes the various relationships among the original data. It is also a method for best approximation of the original data points using fewer dimensions. SVD can be used to make the processing time of WiFall short to achieve automatically fall detection.

SVD is a factorization of a real or complex matrix in linear algebra, and is applied to statistic and signal processing. The basic idea behind SVD is to take a high dimensional, highly variable set of data and then reduce it to a lower dimensional space which exposes the substructure of the original data clearly. The SVD of an $m \times n$ real or complex matrix M is formalized as:

$$M = U\mathbf{\Sigma}V^T, \tag{14}$$

where U is an $m \times m$ real or complex unitary matrix, $\mathbf{\Sigma}$ is an $m \times n$ rectangular diagonal matrix with nonnegative real numbers on the diagonal, and V^T is an $n \times n$ real or complex unitary matrix. We record 100 CSI packages per second, and each package consists of nine stream with each stream having 30 subcarriers. To cover the duration of a whole action (e.g., falling, sitting down), we stack the CSI of two successive seconds together, then obtain a matrix $X \in R^{200\times 270}$ for training and testing. Intuitively, all signal channels are stable in an ideal environment, and will be affected simultaneously by changes in the environment. Consequently, each sample X should be a low-ranking matrix. Fig. 6 plots the eigenvalues of typical samples of different activity classes. As shown, the eigenvalues in all cases decrease rapidly as expected. Moreover, Table 1 shows the proportion of top three eigenvalues in different classes. Interestingly, we discover that the first three sample of the SVD matrix can capture the characteristics of the whole matrix. Therefore, we leverage SVD to select the best three eigenvalues in this matrix to apply classification. Even considering resting as a type of activity, the first 3 eigenvalues from SVD can still provide the features obviously.

4.4 Activity Decision

Two classification algorithms have been applied in WiFall for fall detection. To distinguish falling from the other movements, we first adopt a one-class Support Vector

Machine (SVM) based on the features extracted from profile construction module. To further improve the detection accuracy and to decrease the false alarm, Random Forest (RF) is then applied in WiFall system.

4.4.1 Classification Using a One-Class SVM

To distinguish falling from other movements, a one-class Support Vector Machine is applied. A SVM is a supervised learning model with associated machine learning algorithms which are used to analyze data and recognize patterns. It is one of the most commonly used machine learning tools with strong open-source software supports. A one-class SVM is an extended algorithm of SVM [38]. In a one-class SVM, all the samples are divided into either the objective class or the non-objective class. To solve the nonlinear classification problem, it maps input samples into a high dimensional feature space by using a kernel function and finds the maximum margin hyperplane in the transformed feature space. The hyperplane includes all the objective samples inside and non-objective samples outside.

To figure out the most useful features for classification, we first choose the most frequently used features to characterize the activities, which are normalized standard deviation of CSI, offset of signal strength, period of motion, median absolute deviation, interquartile range, signal entropy, and velocity of signal change. The meaning of the seven features we selected are as follows:

1) Normalized STD: It is related to the dynamic range of the motion.
2) Offset of Signal Strength: It corresponds to the strongest power that is received by MPs.
3) Period of Motion: It shows the time that the activity lasts.
4) Median Absolute Deviation (MAD): MAD is a robust measure of the variability of a univariate sample of quantitative data. The sum of squared MAD can express the concentration of data.
5) Interquartile Range (IR): It corresponds to the dispersion of CSI.
6) Signal Entropy: It is a generic measure of system disorganization.
7) Velocity of Signal Change: Velocity is computed as the first order derivative here, which is an indicator showing how fast the signal is changed by an activity.

Based on the observations in Section 4.2, different streams present different changing patterns when CSI propagation is affected by human activities. To explore the spatial diversity, each stream generates the above seven features respectively and the features together constitute the input of the classification algorithm. The combined feature can represent a comprehensive characteristic of CSI signal variations caused by the activity.

In our application, falling belongs to the objective class, denoted as F. Other human movements belong to the non-objective class. We use LOF to extract the anomaly series and build the classification model by utilizing LibSVM [39]. Then, we apply one-class SVM to assign a label to each group of the test data and recognize human falling from the other activities.

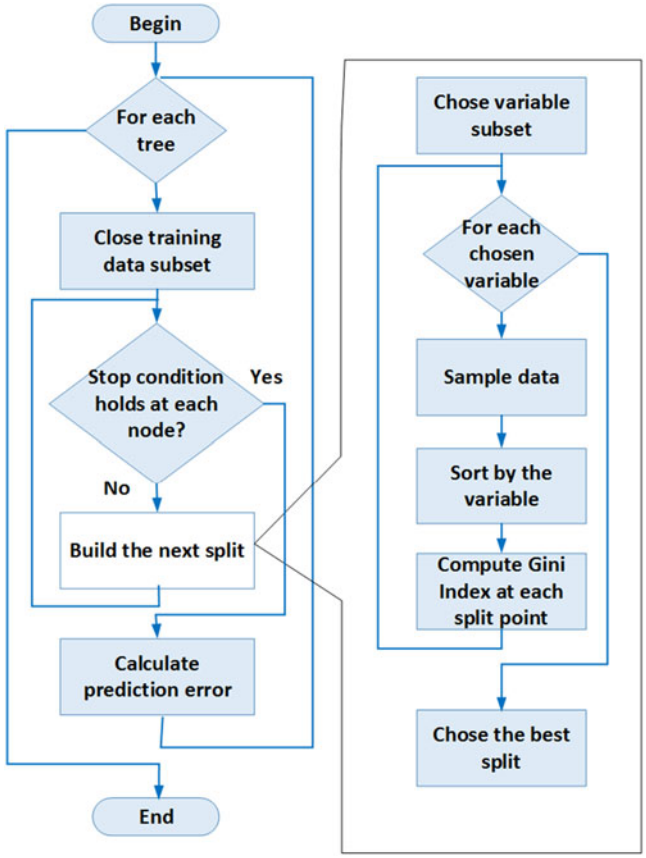

Fig. 7. Random forest flow chart.

4.4.2 Detection Using Random Forests

A one-class SVM classifier is reliable enough to distinguish falling from the other movements, but the fall detection accuracy is not desirable in some environments with rich multipath effects. Meanwhile, we want to extend WiFall to detect more activities rather than falling, one-class SVM is not the optimal solution in this case. Significant improvements in classification accuracy have resulted from growing an ensemble of trees and letting them vote for the classes. As one of the most typical ensemble learning method for classification, Random Forests first construct decision trees at training time and then output the class that is the mode of the classes output by individual trees, and are more likely to improve the detection accuracy. Therefore, we select Random Forests (RF) as the second learning method to build the classification model and improve the accuracy of WiFall.

Fig. 7 is the flow chart of Random Forest algorithm. This classification is used to rank the importance of variables in a classification problem. To measure the variable importance in a dataset $D_n = \{(X_i, Y_i)\}_{i=1}^{n}$, we first fit a random forest to the data. The out-of-bag error for each data point is recorded and averaged over the forest during this process. To measure the importance of the jth feature after training, the values of the jth feature are permuted among the training data and the out-of-bag error is computed on the perturbed dataset. Then we compute an importance score for this feature by averaging the difference in out-of-bag error before and after the permutation over all trees, and the score is normalized by the standard deviation of the difference.

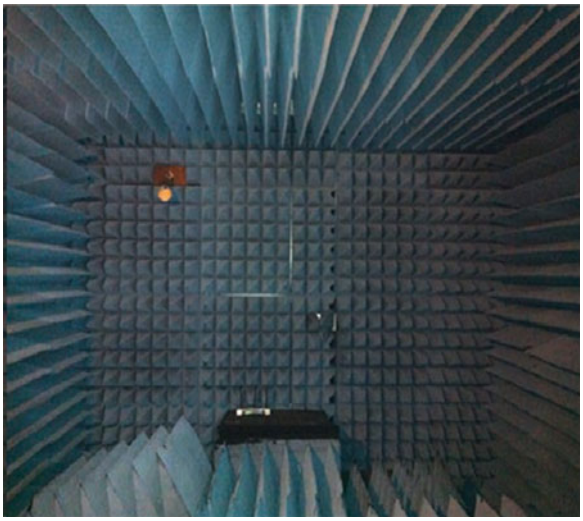

Fig. 8. Scenario 1: Chamber.

Fig. 9. Scenario 2: Laboratory.

We rank the features with large values for this score as more important than the other features. By leveraging the Random Forest algorithm, we can distinguish fall activity from the other activities by comparing the feature importance scores using our selected features, which could improve the fall detection accuracy.

5 Experimental Setup

This section will illustrate the experimental setup and evaluation methods for WiFall. We will present the implementation firstly, followed by the experimental scenarios and evaluation metrics. Then, we analyze the signal properties of different activities and the examination of the effective detection range of a single wireless link. Finally, we will present the performance evaluation method and the user interface of WiFall.

5.1 Implementation

We implement the proposed WiFall system with two TP-LINK TL-WDR7500 wireless routers as the access points (APs), and two 3.20GHz Intel(R) Pentium 4 CPU 2 GB RAM desktops equipped with Intel 5,300 NIC as the monitoring points (MPs). The APs possess 3 detectable antennas, and the MPs have three working antennas and the firmware is modified as in [36] to report CSI to the upper layers. Two APs and MPs form two 3×3 MIMO wireless links and operate on IEEE 802.11n AP mode at 5GHz in order to get free from crowded 2.4GHz interference in the experimental environment. During the experiment, an MP collects CSIs packets from its corresponding AP at the rate of 100 packets per second. CSI packets are collected and sent to one of the two MPs. The MP installed with MATLAB also works as the server to conduct data processing, profile construction, and activity decision.

5.2 Experimental Scenarios

We conduct experiments in three typical indoor environments in the campus of Hong Kong University of Science and Technology, and test different layout schemes. The detailed experimental scenarios are as follows:

- *Chamber.* Chamber in Fig. 8 is an RF shielding system, where wireless signals are absorbed instead of being reflected. Typically, chamber is a free space indoor environment where there is no multipath. It is an ideal environment to test the influence of human activities on CSI. In the chamber, there is only one AP-MP link. AP is settled next to the wall on one side of the chamber, and MP is settled at the opposite side, as shown in Fig. 11.
- *Laboratory.* Experiments are also conducted in an $8m \times 9m$ laboratory as shown in Fig. 9. Since the laboratory is big and spacious, we can test the effective range of one wireless link. In the laboratory, we evaluate the performance of WiFall with two different AP-MP deployments. Figs. 13 and 14 show the AP-MP link(s) deployments.
- *Dormitory.* Finally, we deploy WiFall in a student's dormitory, which is $4m \times 5m$ as shown in Fig. 10. The dormitory scenario is aimed to estimate the indoor environment of a typical living room. We deploy one AP-MP link in the dormitory as shown in Fig. 12.

Fig. 10. Scenario 3: Dormitory.

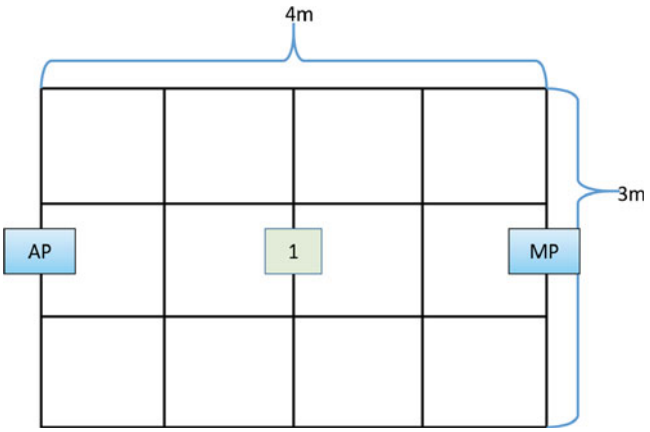

Fig. 11. Link layout and testing locations in the chamber.

5.3 Evaluation Metrics

Two metrics are introduced to analyze the performance of WiFall: detection rate (DR_{fall}) and false alarm (FA_{fall}). DR_{fall} is the probability that WiFall system can detect falling movement, which is computed as:

$$DR_{fall} = \frac{number\ of\ truly\ detected\ fall}{number\ of\ total\ fall}. \quad (15)$$

FA_{fall} refers to the proportion that the system generates an alarm when there is no fall happens, which is computed as:

$$FA_{fall} = \frac{number\ of\ wrongly\ detected\ fall}{number\ of\ total\ fall}. \quad (16)$$

5.4 Evaluation Schemes

We design different evaluation schemes in the three experimental scenarios. During the experiment, one person performs as the user of WiFall and conducts the specific activities in the area of interest. We involve another person as the handler to monitor the action of the WiFall user. The handler should stay outside the area of interest. The handler labels the received CSI data manually every second during monitoring. When hearing the instructions from the handler, the user of WiFall performs action promptly.

In the chamber, we test sitting down, standing up and falling. These three kinds of activities are similar, so it is hard to distinguish falling from the others. The experiment conducted in chamber is aimed to figure out whether we can leverage CSI variations caused by different movements to recognize human falling. During experiment, only one male person performs each of the selected activities in the middle of the chamber for 50 times.

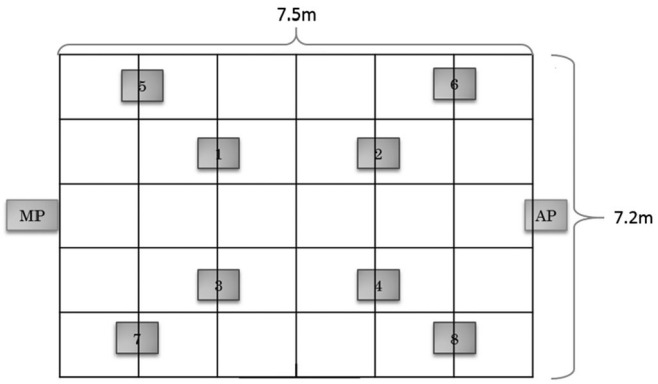

Fig. 13. Link layout and testing locations in the laboratory with one AP-MP link.

In the laboratory, the activities tested in the laboratory are walking, standing up, sitting down, and falling. We both consider long-time walking and short-time walking in our experiment. The long-time walking means that the person walks for 1 minute and longer. The short-time walking means that the person walks for several seconds (e.g., 10s, 15s, etc.) and then stops. Ten students (eight male and two female) with different heights and weights participate in data collection. Each of them performs each activity at eight different locations shown in Fig. 13 for 200 times (25 times at each location).

We also test the prediction accuracies of all activity classifications in the dormitory environment. The activities tested in dormitory are the same with those in laboratory. We only consider short-time walking in dormitory, and we require that the person is resting before and after performing other three activities. We randomly select five locations as the testing location, shown in Fig. 12. To collect training data, eight people conduct all the activities in the dormitory, and each of them performs each of the activity for 100 times (20 times at each location).

5.5 User Interface

We implement the user interface of WiFall and conduct real scenario experiments in the dormitory. The server side of

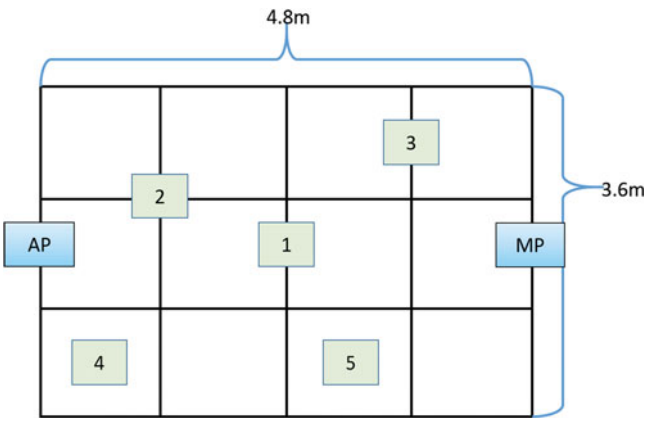

Fig. 12. Link layout and testing locations in the dormitory.

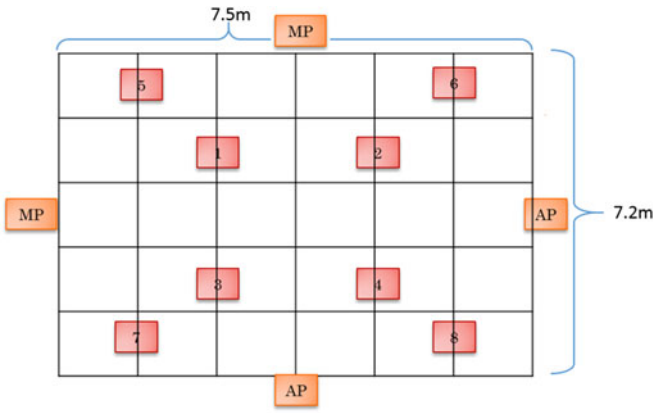

Fig. 14. Link layout and testing locations in the laboratory with two AP-MP links

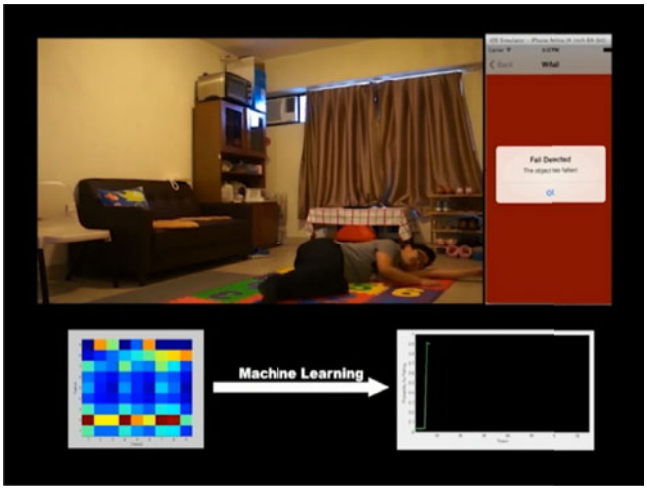

Fig. 15. User interface of WiFall with falling probability.

WiFall is implemented using MATLAB showing the probability of falling at the time unit, as shown in the bottom right of Fig. 15. We also implement a client user interface under IOS operating system, as shown in the upper right of Fig. 15. When a fall of the object person is detected, WiFall server will send alarm signal to the client. WiFall client provides the users with the current activity information and alarms the users if a the fall alarm signal is received.

6 Performance Evaluation

In this section, we present the evaluation results of WiFall systems. We first show evaluation results of anomaly detection using LOF, and analyze the effective range of an AP-MP link. Then, we present how the height of an AP-MP link will impact on fall detection accuracy. Finally, we present the overall evaluation result of WiFall.

6.1 Anomaly Detection with LOF

Anomaly activities are detected using LOF. Since multipath will cause differences in time delay, amplitude attenuation and phase shifts, MP will receive several different signal strengths from the same AP through multiple paths. The signal strength with the longest time delay and weakest power will usually be ignored. If a falling movement occurs far from APs and MPs, the changes of the partially received signal power may not be able to detect the movement. In this part, we evaluate anomaly detection using LOF, and define the effective range of an AP-MP link for activity detection based on our observation.

We conduct experiments in the laboratory to evaluate anomaly detection. We examine whether an anomaly can be detected using LOF effectively when the distance from LOS is increased and determine the effective range. The distances from the person and the LOS path are selected as $1.5m$, $2m$, $2.5m$ and $3m$. For each distance, we uniformly select eight locations (total 32 NLOS locations) for testing. The distance between two successive locations at one side is $1.5m$. When the person performs an activity, LOF will change significantly as shown in Fig. 16. Compared with the other two in-place activities, walking leads to a more obvious change in LOF values, since the location of the person keeps changing. Thus walking is much

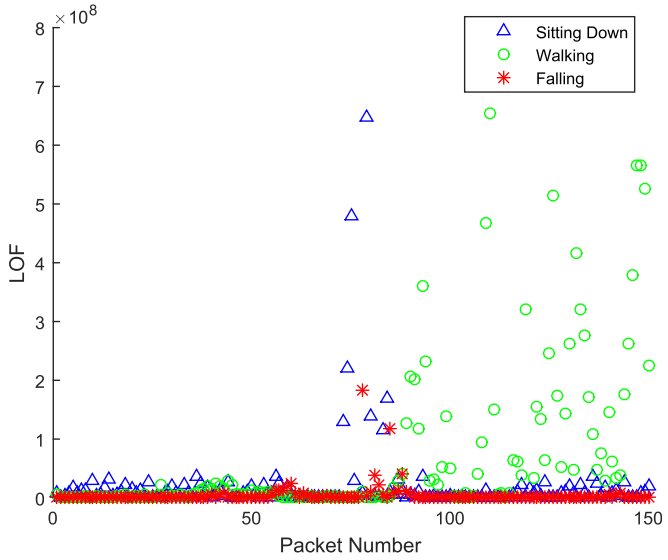

Fig. 16. LOF values of different activities.

easier to be detected than the other in-place activities as anomaly by WiFall.

Two metrics are introduced to evaluate the anomaly detection accuracy. The Detection Rate ($DR_{anomaly}$) is computed as:

$$DR_{anomaly} = \frac{number\ of\ detected\ anomaly}{number\ of\ total\ anomaly}. \quad (17)$$

The false alarm of anomaly detection is defined as:

$$FA_{anomaly} = \frac{number\ of\ wrongly\ detected\ anomaly}{number\ of\ normal\ activity}. \quad (18)$$

Fig. 17 shows the anomaly detection rate using LOF. When the activities happen within $1.5m$ from the line of sight path, 100 percent of $DR_{anomaly}$ can be achieved. When the distance increases to $2.5m$, $DR_{anomaly}$ decreases to 87 percent. When the distance is increased to $3m$, the $DR_{anomaly}$ is 84 percent. Consider the detection rate along LOS at distance $3m$, the rate of the middle two locations at one side is 89 percent, the rate of the other two locations is

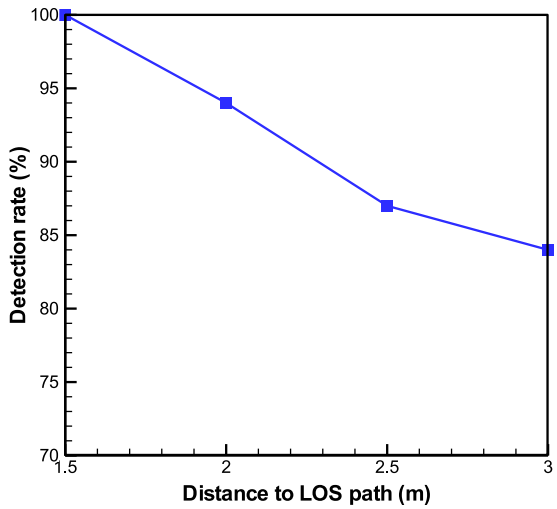

Fig. 17. Anomaly DR when distance to LOS increases.

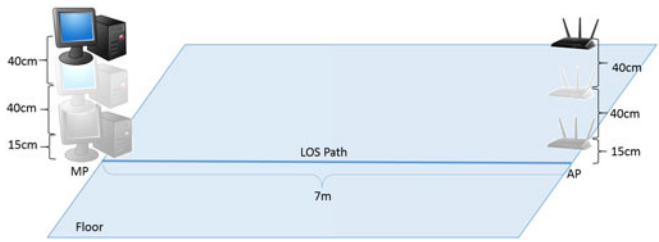

Fig. 18. AP-MP link placement with different heights.

78 percent. Meanwhile, we also observe that when a person is resting at one of the selected 32 locations, anomaly is detected only twice among the 128 tests, which means the false alarm of LOF is less than 2 percent. From the evaluation results we can determine the effective range of WiFall. Since the coverage of wireless signal will be wider when the transmission power of the AP increases, we can leverage power control method to increase the signal transmission power of WiFall AP, thus increase the effective range. Due to the fact that the elderly always stay in a specific room and the size of the rooms are limited, the effective range of WiFall can cover the range of activities for the elderly.

6.2 Height of AP-MP Link

During falling, the position of the person will change significantly in the vertical plane. Therefore, the height of an AP-MP link may affect the fall detection accuracy. To find the link height which can provide most precise detection accuracy, we test WiFall with AP-MP placements at different heights. As shown in Fig. 18, we set the AP-MP link at three heights: $0.15m$, $0.55m$, and $0.95m$. We ask three people to conduct the experiment. During the experiment, one of the three people performs the activities (e.g., falling, standing up, etc.) on LOS and NLOS path. The farthest distance from the person's location and LOS path is $1m$. We evaluate the activity classification accuracy using RF learning algorithm after SVD matrix factorization. Fig. 19 shows the evaluation results at different heights. When AP-MP is set at $0.55m$, WiFall can achieve best detection accuracy for all the activities. Therefore, we select $0.55m$ as the height for our AP-MP placement, and use this height in our following experiments.

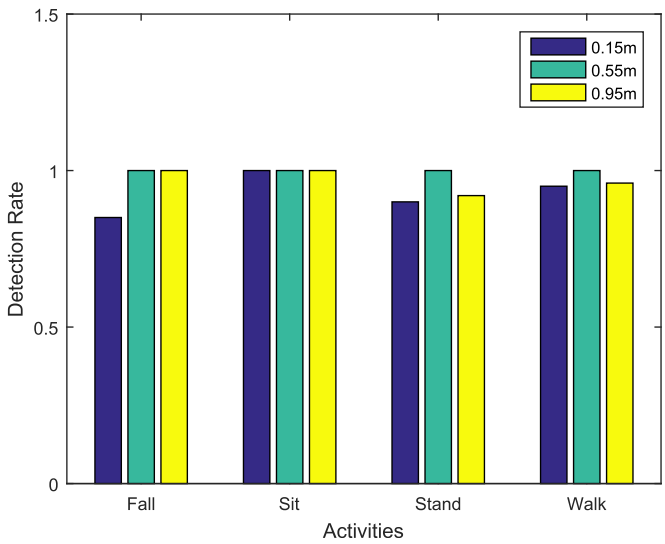

Fig. 19. Detection rates at different heights.

TABLE 2
Experiment Results with One-Class SVM

	Precision	False Alarm
chamber	96%	18%
laboratory-one link	88%	16%
laboratory-two links	94%	11%
dormitory	83%	14%

6.3 Performance of WiFall

In this section, we evaluate WiFall using RF and SVD, and compare the result with the performance in [19].

Table 2 shows the fall detection results using a one-class SVM classifier with seven selected features from [19]. Table 3 shows the evaluation results using an RF classifier with SVD matrix factorization. Compared the results using RF and SVD with the results of previous WiFall version, we observe that new version of WiFall can achieve better performance in all the experimental scenarios. This is one of the most important reasons that we choose this Random Forest as the algorithm for WiFall systems.

Meanwhile, we also observe that the false alarm of new WiFall system is still above 10 percent. The major reason of the high false alarm is that our dataset for falling is limited currently. By using a larger training dataset, we can improve the performance of WiFall and decrease the false alarm. The feedback data from alerting phase can be utilized to gradually enrich the training database.

Another reason of high false alarm is that we mark the label of different activities manually, and the labeling rate is much lower than the CSI sampling rate. From our experimental setting, we receive one CSI packet every 0.01s. However, the handler person cannot label the data every 0.01s. So, we ask the person to label the data of every 1s. It is reasonable that the label we give should represent the corresponding activity of the majority of data. By strictly control the experiment process, only a small number of errors will occur when the label represents the corresponding activity of the minority of data. This is because that different WiFall user will show different response time. We cannot thoroughly eliminate this uncontrollable factor, but we can reduce the error probability caused by this reason with automatic labeling. If we can automatically label the data at the CSI sampling rate, we can apply a simple algorithm to elect the label of the majority data, and then consider it to be the label of the data in 1 second. It will help to decrease the false alarm rate. We are now searching for an automatic labeling method to decrease the false alarm.

We also observe that the location of the target person will slightly affect the performance of WiFall. We divide the eight locations in Fig. 13 into two groups (Group 1: 1/2/3/4, Group 2: 5/6/7/8) and test the activity detection ratio with

TABLE 3
Experiment Results with Random Forest

	Precision	False Alarm
chamber	98%	15%
laboratory-one link	93%	13%
laboratory-two links	96%	10%
dormitory	89%	12%

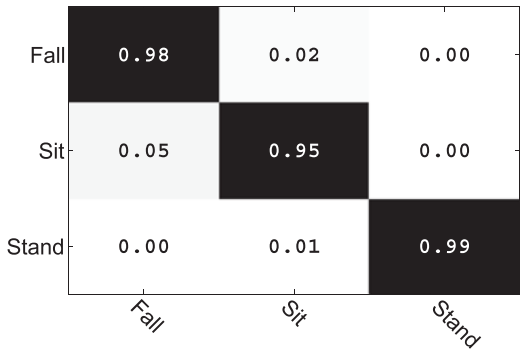

Fig. 20. Confusion matrix when user does actions at location 1, 2, 3, 4.

one AP-MP link in the laboratory. Since the location of the person keeps changing during walking, we only consider the three in-place activities (falling, sitting down, and standing up) and test the performance using RF. Figs. 20 and 21 show the evaluation results at the locations 1/2/3/4 and at 5/6/7/8. We observe that when the action locations are closer to the AP-MP link, the performance of WiFall is better. During standing up, the body of the user changes from a lower position to an upper position, which is obviously different from the other two activities. Therefore, we discover that standing up can be distinguished easily.

Falling after resting or walking may have different impact on signal propagation, thus influence the fall detection rate. We want to ensure that WiFall can keep a satisfactory detection accuracy throughout. From previous experiment, we observe that long-time walking and short-time walking will not affect the fall detection rate. Since the size of the room is limited, the walking considered in this evaluation is short-time walking. Fig. 22 shows the evaluation result considering more specific activities (resting-falling, resting-sitting, resting-walking, walking-falling, walking-sitting and walking-resting) at LOS path. When we only consider the activities starting from resting, the average activity classification rate is 98 percent. When we consider activities starting from resting (e.g., resting-falling) and those starting from walking (e.g., walking-falling) together, the rate decrease to 86 percent.

We also evaluate the performance of WiFall when the AP-MP link in the lab is blocked. We use a desk to block the LOS path of the AP-MP link, and asks volunteers to conduct activities at both LOS and NLOS locations. Fig. 23 shows that when the AP-MP link is blocked by the desk, the fall detection rate decreases to around 60 percent both at LOS

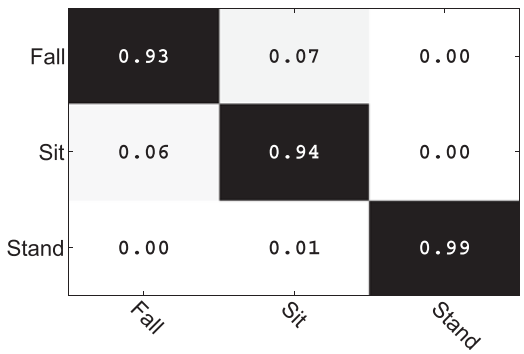

Fig. 21. Confusion matrix when user does actions at location 5, 6, 7, 8.

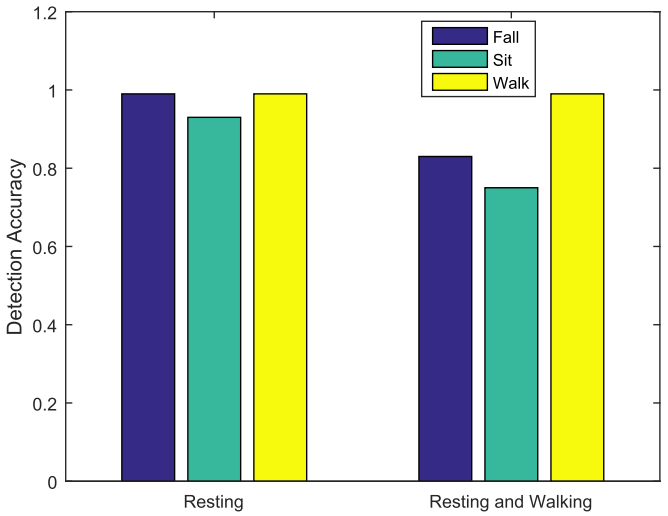

Fig. 22. Detection rates of activities from different status.

and NLOS locations. The detection rate of other activities also decrease. However, we still believe that WiFall can be widely deployed since furniture is always placed at the corner of a room where AP-MP link may not be blocked.

6.4 Efficiency of SVD Matrix Factorization

We also evaluate the time efficiency using SVD matrix factorization. We select a 166 MB CSI dataset and use RF to classify the activities with or without using SVD. The dataset contains 48 test cases of three different activities at four locations. As shown in Fig. 24, the average time to process the data for activity classification without or with SVD are 211.4s and 35.9s, respectively. The speedup using SVD is 5.89. Using SVD matrix factorization, it takes less than 0.75s to identify the activity of a test case, which proves that WiFall is able to support online activity monitoring. From this, we can conclude that SVD can highly reduce the processing time, thus achieve automatic fall detection.

7 Conclusions and Discussions

In this paper, we propose WiFall, a device-free fall detection system leveraging Channel State Information as the

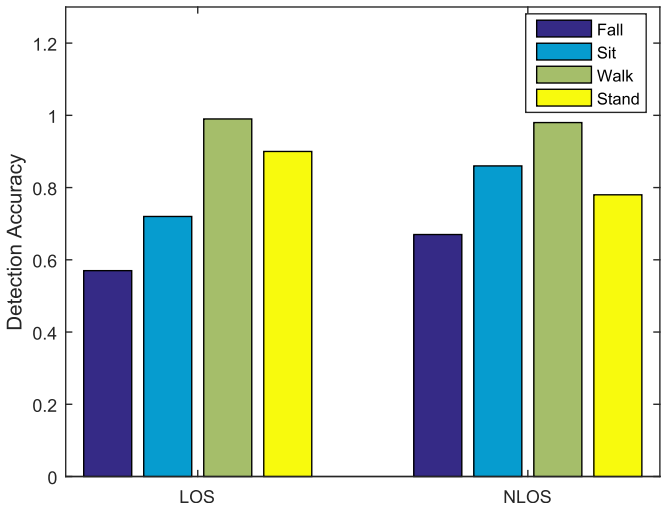

Fig. 23. Performance of WiFall when AP-MP link is blocked.

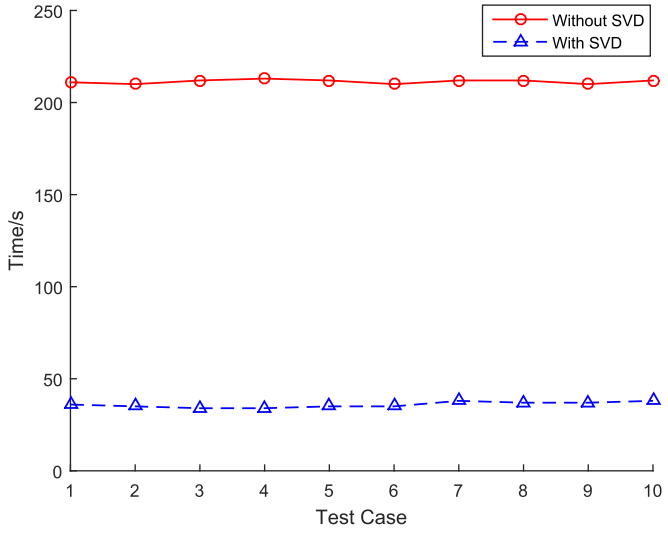

Fig. 24. Processing time with or without SVD.

indicator. WiFall aims to detect the fall of the elderly, and can also identify some other activities. WiFall takes advantages of the physical layer Channel State Information in widely deployed off-the-shelf WiFi infrastructure. To demonstrate the feasibility and effectiveness, we implement the WiFall servers on laptops with commodity 802.11n NICs and conduct comprehensive experiment in three different scenarios with various Tx-Rx layouts. Experimental results show that WiFall can achieve an satisfactory fall detection accuracy with acceptable false alarm rate.

At the present stage, WiFall can effectively identify the most common daily activities such as walking, sitting down, standing up, and falling. More specific activities will be considered in our future work. Same with other device-free activity recognition systems using wireless signals, WiFall is currently designed for and tested with only one single person in the area of interest. Currently, it is difficult to identify the activity of a person among multiple users. When multiple people are conducting different activities, their movements will cause mutual influence to the signal propagation. Considering an easier case, when only one person is conducting activities, the locations of other objects will also influence the signal propagation paths. Therefore, it is nontrivial to propose a thorough propagation model considering the relationship between signal variation and multiple human activities. Meanwhile, it is too costly to build the training database using learning methods since there are various combinations when considering different numbers, activities and locations of objects. Nevertheless, we still believe that WiFall can be applied to important use cases, and will greatly contribute to the human healthcare industry with wireless techniques.

Acknowledgments

This research is supported in part by Guangdong Natural Science Funds for Distinguished Young Scholar (No. S20120011468), the Shenzhen Science and Technology Foundation (No. JCYJ20140509172719309, KQCX20150324160536457), China NSFC Grant 61472259, 61370185, GDUPS (2015), Guangdong Young Talent Project 2014TQ01X238, and Hong Kong RGC Grant HKUST16207714 and the University of Macau Grant SRG2015-00050-FST. Kaishun Wu is the corresponding author.

References

[1] N. Noury, A. Fleury, P. Rumeau, A. Bourke, G. Laighin, V. Rialle, and J. Lundy, "Fall detection-principles and methods," in *Proc. 29th Annu. Int. Conf. Eng. Med. Biolo. Soc.*, 2007, pp. 1663–1666.

[2] CDC, "Falls among older adults: An overview," 2013, (Apr.). [Online]. Available: http://www.cdc.gov/HomeandRecreationalSafety/Falls/adultfalls.html

[3] M. Alwan, P. J. Rajendran, S. Kell, D. Mack, S. Dalal, M. Wolfe, and R. Felder, "A smart and passive floor-vibration based fall detector for elderly," in *Proc. 2nd Int. Conf. Inform. Commun. Technol.*, vol. 1, pp. 1003–1007, 2006.

[4] H. Rimminen, J. Lindstrom, M. Linnavuo, and R. Sepponen, "Detection of falls among the elderly by a floor sensor using the electric near field," *IEEE Trans. Inform. Technol. Biomed.*, vol. 14, no. 6, pp. 1475–1476, Nov. 2010.

[5] H. Foroughi, A. Naseri, A. Saberi, and H. S. Yazdi, "An eigenspace-based approach for human fall detection using integrated time motion image and neural network," in *Proc. 9th Int. Conf. Signal Process.*, 2008, pp. 1499–1503.

[6] H. Foroughi, B. S. Aski, and H. Pourreza, "Intelligent video surveillance for monitoring fall detection of elderly in home environments," in *Proc. 11th Int. Conf. Comput. Inform. Technol.*, 2008, pp. 219–224.

[7] F. Bianchi, S. J. Redmond, M. R. Narayanan, S. Cerutti, and N. H. Lovell, "Barometric pressure and triaxial accelerometry-based falls event detection," *IEEE Trans. Neural Syst. Rehabil. Eng.*, vol. 18, no. 6, pp. 619–627, Dec. 2010.

[8] J. Dai, X. Bai, Z. Yang, Z. Shen, and D. Xuan, "Perfalld: A pervasive fall detection system using mobile phones," in *Proc. 8th IEEE Int. Conf. Pervasive Comput. Commun. Workshops*, 2010, pp. 292–297.

[9] K. Wu, J. Xiao, Y. Yi, M. Gao, and L. M. Ni, "Fila: Fine-grained indoor localization," in *Proc. INFOCOM*, 2012, pp. 2210–2218.

[10] J. Xiao, K. Wu, Y. Yi, L. Wang, and L. M. Ni, "Fimd: Fine-grained device-free motion detection," in *Proc. IEEE 18th Int. Conf. Parallel Distrib. Syst.*, 2012, pp. 229–235.

[11] D. Zhang, J. Ma, Q. Chen, and L. M. Ni, "An rf-based system for tracking transceiver-free objects," in *Proc. 5th Annu. IEEE Int. Conf. Pervasive Comput. Commun.*, 2007, pp. 135–144.

[12] X. Yu, "Approaches and principles of fall detection for elderly and patient," in *Proc. 10th Int. Conf. e-health Netw., Appl. Serv., HealthCom*, 2008, pp. 42–47.

[13] M. Mubashir, L. Shao, and L. Seed, "A survey on fall detection: Principles and approaches," *Neurocomputing*, vol. 100, pp. 144–152, Jan. 2013.

[14] F. Adib and D. Katabi, "See through walls with wifi!" in *Proc. ACM SIGCOMM Conf. SIGCOMM*, 2013, pp. 75–86.

[15] F. Adib, Z. Kabelac, D. Katabi, and R. C. Miller, "3d tracking via body radio reflections," in *Proc. 11th USENIX Conf. Netw. Syst. Des. Implementation*, 2014, vol. 14, pp. 317–329.

[16] F. Adib, Z. Kabelac, and D. Katabi, "Multi-person localization via RF body reflections," in *Proc. 12th USENIX Conf. Netw. Syst. Des. Implementation*, 2015, pp. 279–292.

[17] Q. Pu, S. Gupta, S. Gollakota, and S. Patel, "Whole-home gesture recognition using wireless signals," in *Proc. 19th Annu. Int. Conf. Mobile Comput. Netw.*, 2013, pp. 27–38.

[18] H. Abdelnasser, M. Youssef, and K. A. Harras, "Wigest: A ubiquitous wifi-based gesture recognition system," *arXiv:1501.04301*, 2015.

[19] C. Han, K. Wu, Y. Wang, and L. M. Ni, "Wifall: Device-free fall detection by wireless networks," in *Proc. INFOCOM*, 2014, pp. 271–279.

[20] Y. Wang, J. Liu, Y. Chen, M. Gruteser, J. Yang, and H. Liu, "E-eyes: Device-free location-oriented activity identification using fine-grained wifi signatures," in *Proc. 20th Annu. Int. Conf. Mobile Comput. Netw.*, 2014, pp. 617–628.

[21] B. Wei, W. Hu, M. Yang, and C. T. Chou, "Radio-based device-free activity recognition with radio frequency interference," in *Proc. 14th Int. Conf. Inform. Process. Sens. Netw.*, 2015, pp. 154–165.

[22] W. Wang, A. X. Liu, M. Shahzad, K. Ling, and S. Lu, "Understanding and modeling of wifi signal based human activity recognition," in *Proc. 21st Annu. Int. Conf. Mobile Comput. Netw.*, 2015, pp. 65–76.

[23] W. He, K. Wu, Y. Zou, and Z. Ming, "Wig: Wifi-based gesture recognition system," in *Proc. 24th Int. Conf. Comput. Commun. Netw.*, 2015, pp. 1–7.
[24] K. Ali, A. X. Liu, W. Wang, and M. Shahzad, "Keystroke recognition using wifi signals," in *Proc. 21st Annu. Int. Conf. Mobile Comput. Netw.*, 2015, pp. 90–102.
[25] L. Sun, S. Sen, D. Koutsonikolas, and K.-H. Kim, "Widraw: Enabling hands-free drawing in the air on commodity wifi devices," in *Proc. 21st Annu. Int. Conf. Mobile Comput. Netw.*, 2015, pp. 77–89.
[26] M. Youssef, M. Mah, and A. Agrawala, "Challenges: Device-free passive localization for wireless environments," in *Proc. 13th Annu. ACM Int. Conf. Mobile Comput. Netw.*, 2007, pp. 222–229.
[27] M. Seifeldin, A. Saeed, A. E. Kosba, A. El-Keyi, and M. Youssef, "Nuzzer: A large-scale device-free passive localization system for wireless environments," *IEEE Trans. Mobile Comput.*, vol. 12, no. 7, pp. 1321–1334, Jul. 2013.
[28] I. Sabek, M. Youssef, and A. V. Vasilakos, "Ace: An accurate and efficient multi-entity device-free wlan localization system," *IEEE Trans. Mobile Comput.*, vol. 14, no. 2, pp. 261–273, Feb. 2015.
[29] K. Wu, J. Xiao, Y. Yi, D. Chen, X. Luo, and L. M. Ni, "Csi-based indoor localization," *IEEE Trans. Parallel Distrib. Syst.*, vol. 24, no. 7, pp. 1300–1309, Jul. 2013.
[30] X. Guo, D. Zhang, K. Wu, and L. M. Ni, "Modloc: Localizing multiple objects in dynamic indoor environment," *IEEE Trans. Parallel Distrib. Syst.*, vol. 25, no. 11, pp. 2969–2980, Nov. 2014.
[31] J. Xiao, K. Wu, Y. Yi, L. Wang, and L. M. Ni, "Pilot: Passive device-free indoor localization using channel state information," in *Proc. IEEE 33rd Int. Conf. Distrib. Comput. Syst.*, 2013, pp. 236–245.
[32] H. Abdel-Nasser, R. Samir, I. Sabek, and M. Youssef, "Monophy: Mono-stream-based device-free wlan localization via physical layer information," in *Proc. Wireless Commun. Netw. Conf.*, 2013, pp. 4546–4551.
[33] W. Yang, L. Gong, D. Man, J. Lv, H. Cai, X. Zhou, and Z. Yang, "Enhancing the performance of indoor device-free passive localization," *Int. J. Distrib. Sens. Netw.*, vol. 501, p. 256162, 2015.
[34] Z. Yang, Z. Zhou, and Y. Liu, "From RSSI to CSI: Indoor localization via channel response," *ACM Comput. Surveys*, vol. 46, no. 2, p. 25, 2013.
[35] D. M. Pozar, *Microwave Engineering*. New York, NY, USA: Wiley, 2009.
[36] D. Halperin, W. Hu, A. Sheth, and D. Wetherall, "Tool release: Gathering 802.11 n traces with channel state information," *ACM SIGCOMM Comput. Commun. Review*, vol. 41, no. 1, pp. 53–53, 2011.
[37] M. M. Breunig, H.-P. Kriegel, R. T. Ng, and J. Sander, "Lof: Identifying density-based local outliers," in *ACM Sigmod Rec.*, vol. 29, no. 2, 2000, pp. 93–104.
[38] B. Schölkopf, J. C. Platt, J. Shawe-Taylor, A. J. Smola, and R. C. Williamson, "Estimating the support of a high-dimensional distribution," *Neural Comput.*, vol. 13, no. 7, pp. 1443–1471, 2001.
[39] C.-C. Chang and C.-J. Lin, "Libsvm: A library for support vector machines," *ACM Trans. Intell. Syst. Technol.*, vol. 2, no. 3, p. 27, 2011.

Yuxi Wang received the BEng degree in compute engineering from the Hong Kong University of Science and Technology (HKUST) in 2013, and is currently working toward the PhD degree in computer science and engineering at HKUST. Her research interests include wireless communication, mobile computing, and wireless sensor networks. She is a student member of the IEEE.

Kaishun Wu received the PhD degree in computer science and engineering from the Hong Kong University of Science and Technology, in 2011. After that, he worked as a research assistant professor at the Hong Kong University of Science and Technology. In 2013, he joined Shenzhen University as a distinguished professor. He has co-authored two books and published more than 80 refereed papers in international leading journals and premiere conferences. He is the inventor of 6 US and 43 Chinese pending patents (13 are issued). He won the best paper awards at IEEE Globecom 2012, IEEE ICPADS 2012, and IEEE MASS 2014. He received the 2014 IEEE ComSoc Asia-Pacific Outstanding Young Researcher Award and was selected as 1,000 Talent Plan for Young Researchers. He is a member of the IEEE.

Lionel M. Ni received the PhD degree in electrical and computer engineering from Purdue University in 1980. He is a chair professor in the Department of Computer and Information Science and Vice Rector of Academic Affairs at the University of Macau. Previously, he was a chair professor of computer science and engineering at the Hong Kong University of Science and Technology. As a fellow of the IEEE and Hong Kong Academy of Engineering Science, he has chaired more than 30 professional conferences and has received eight awards for authoring outstanding papers.